Bulletin of the Seismological Society of America, Vol. 69, No. 6, pp. 1851–1859, December 1979

MECHANISM OF THE MAIN SHOCK AND THE AFTERSHOCK STUDY OF THE TABAS-E-GOLSHAN (IRAN) EARTHQUAKE OF SEPTEMBER 16, 1978: A PRELIMINARY REPORT

BY M. BERBERIAN,* I. ASUDEH, R. G. BILHAM, C. H. SCHOLZ, AND C. SOUFLERIS

ABSTRACT

Aftershocks of the Tabas-e-Golshan earthquake (M_S = 7.7) of September 16, 1978 were recorded with a local network of portable seismometers. The main shock produced a discontinuous series of surface ruptures extending 85 km NNW and dipping ENE beneath the Shotori Range. The largest aftershocks located thus far are not concentrated in the hypocentral region of the main shock nor near the ends of the rupture zone but appear to be concentrated down-dip from gaps in the surface ruptures. This suggests that these features may extend to depth and act as barrier zones in the rupture process.

The 65 km long zone of aftershock activity dips 40°ENE from the surface break, which agrees with the focal mechanism for the main shock in indicating thrusting on a NNW-striking, ENE-dipping fault. The aftershocks range in depth from 2 to 24 km with greatest concentration in the depth range 5 to 10 km.

INTRODUCTION

The Tabas-e-Golshan earthquake of magnitude M_S = 7.7 occurred in east central Iran on September 16, 1978 at 15.36.56 UTC. The main shock destroyed or severely damaged about 90 villages, slightly damaged 50 more, and completely demolished the town the Tabas where 85 per cent of the population were killed. In total, the shock killed over 20,000 people, injured thousands, and destroyed over 15,000 housing units and 30 qanats (Berberian, 1979a). Surface rupture occurred along a major existing but hitherto unrecognized Quaternary fault. The rupture extended for about 85 km in eight separated segments with no visible connection at the surface along a general NW-SE trend. The active fault was a thrust at the base of a series of low hills made up of Neogene clay deposits which separates the Shotori horst from the Tabas compressional depression. The minimum vertical uplift and total slip are about 150 and 300 cm, respectively (Berberian, 1979b).

A team from the University of Cambridge, the Lamont-Doherty Geological Observatory of Columbia University, and the Geological and Mineral Survey of Iran arrived in the area 10 days after the main shock. The field work lasted 40 days and, in this period, the earthquake fault was mapped and aftershocks were recorded by an array of nine seismometers operated for 30 days. This is a preliminary note on a few larger aftershocks; an investigation of the whole data set is in progress. The instruments used were five Sprengnether MEQ-800, four Lamont big drum seismographs with L4 1-Hz and Willmore Mk II vertical component seismometers, and three Kinemetrics strong-motion instruments. The Sprengnethers were operated at 66 and 72 dB and the recording speeds used were 60 mm/min for the MEQ 800, giving a 24-hr record and 120 mm/min for the Lamont big drum recorders, giving a 48-hr record. Timing was maintained within 0.02 sec from a radio time signal (usually Moscow). An initial investigation of the length and mechanism of the surface break served as a guide in selecting the instrument positions. With the first available data, and during the whole recording period, selected earthquakes were

* On leave of absence from Tectonic-Seismotectonic Research Section, Geological and Mineral Survey of Iran, P.O. Box 1964, Tehran-Iran.

TABLE 1

HYPOCENTRAL PARAMETERS OF THE 62 LARGER AFTERSHOCKS OF THE TABAS-E-GOLSHAN EARTHQUAKE TOGETHER WITH EPICENTER AND FOCAL DEPTH ERRORS

NO	LAT	LON	STANDARD DEVIATION	FOCAL DEPTH (KM)	FOC.DP. ERROR (KM)	ORIGIN TIME (GMT)	DATE DY.MT.YEAR
01	33.628	56.998	0.09	11.07	1.77	09:20:25:80	03.10.1978
02	33.575	57.070	0.27	06.18	1.47	10:42:35:21	03.10.1978
03	33.283	57.325	0.24	10.54	2.25	14:02:13:66	03.10.1978
04	33.688	57.075	0.20	08.55	2.12	14:04:32:01	03.10.1978
05	33.772	57.130	0.17	14.78	2.64	17:03:44:24	03.10.1978
06	33.438	57.041	0.53	04.71	2.14	21:02:55:56	03.10.1978
07	33.457	57.175	0.24	10.44	2.05	21:34:58:81	03.10.1978
08	33.652	57.003	0.26	06.65	1.25	23:54:15:31	03.10.1978
09	33.495	57.050	0.44	05.86	1.81	03:48:51:13	04.10.1978
10	33.625	57.043	0.12	06.38	0.65	06:33:30:09	04.!0.1978
11	33.345	56.993	0.17	07.00	0.67	11:27:31:48	04.10.1978
12	33.473	57.098	0.59	04.94	1.69	12:30:09:34	04.10.1978
13	33.288	57.063	0.27	06.01	1.05	13:49:27:47	04.10.1978
14	33.350	57.025	0.30	08.48	2.64	13:52:18:36	04.10.1978
15	33.653	57.058	0.21	08.69	1.68	14:07:52:77	04.10.1978
16	33.661	57.068	0.23	08.44	3.19	14:24:46:94	04.10.1978
17	33.422	57.093	0.28	13.77	2.40	16:24:55:71	04.10.1978
18	33.467	57.205	0.39	12.93	3.73	19:11:59:56	04.10.1978
19	33.492	56.997	0.27	02.92	1.21	21:49:54:81	04.10.1978
20	33.657	57.048	0.34	04.12	1.69	00:35:03:08	05.10.1978
21	33.642	57.077	0.02	09.99	0.18	01:37:57:52	05.10.1978
22	33.445	57.232	0.41	09.52	1.84	08:47:08:60	05.10.1978
23	33.637	57.047	0.39	09.43	2.80	09:14:12:61	05.10.1978
24	33.495	57.292	0.30	02.34	1.63	12:23:24:11	05.10.1978
25	33.682	57.095	0.27	11.06	3.14	12:58:21:55	05.10.1978
26	33.590	57.227	0.03	04.42	0.13	15:39:05:84	05.10.1978
27	33.310	56.820	0.11	10.83	2.16	16:02:13:21	05.10.1978
28	33.580	57.110	0.31	08.01	2.05	17:31:25:15	05.10.1978

29	33.250	56.967	0.26	02.12	1.27	18:06:21:64	05.10.1978
30	33.318	57.095	0.38	05.93	1.55	18:27:05:88	05.10.1978
31	33.633	57.065	0.09	05.72	0.29	01:42:37:99	06.10.1978
32	33.387	56.963	0.13	04.30	0.45	04:52:41:50	06.10.1978
33	33.542	57.072	0.16	06.24	0.76	06:38:26:13	06.10.1978
34	33.563	57.078	0.20	10.30	1.11	08:30:50:86	06.10.1978
35	33.393	56.953	0.33	16.62	2.99	10:34:15:18	06.10.1978
36	33.370	57.237	0.30	22.43	2.88	10:59:18:61	06.10.1978
37	33.562	57.103	0.33	13.51	3.38	12:37:54:47	06.10.1978
38	33.448	57.203	0.32	18.13	3.16	13:14:29:81	06.10.1978
39	33.447	57.055	0.34	12.77	2.47	00:06:02:39	07.10.1978
40	33.673	57.122	0.22	12.28	2.47	04:08:37:24	07.10.1978
41	33.650	57.088	0.34	06.64	1.41	12:33:47:12	07.10.1978
42	33.398	56.877	0.20	16.67	1.01	21:25:06:81	07.10.1978
43	33.656	57.160	0.25	10.09	1.68	02:13:21:22	08.10.1978
44	33.598	57.072	0.14	08.63	0.92	04:12:01:95	08.10.1978
45	33.353	57.356	0.16	04.13	0.72	05:40:58:36	08.10.1978
46	33.280	57.067	0.10	06.64	0.51	06:02:01:79	08.10.1978
47	33.690	57.035	0.20	14.20	2.63	12:18:42:47	08.10.1978
48	33.310	57.180	0.25	13.86	3.12	15:19:33:63	08.10.1978
49	33.312	57.288	0.13	11.60	1.84	15:58:42:98	08.10.1978
50	33.330	57.470	0.17	09.95	1.68	22:13:36:56	08.10.1978
51	33.305	57.305	0.26	12.53	3.43	23:25:18:31	08.10.1978
52	33.265	57.238	0.37	06.64	1.52	00:42:46:74	09.10.1978
53	33.330	57.290	0.21	13.39	3.02	13:19:34:07	09.10.1978
54	33.533	57.077	0.26	12.58	3.15	13.39.04:64	09.10.1978
55	33.407	57.065	0.27	17.09	3.24	17:51:36:89	09.10.1978
56	33.247	57.350	0.22	24.06	3.41	18:52:10:44	09.10.1978
57	33.373	57.010	0.21	22.77	2.04	06:42:01:76	10.10.1978
58	33.388	57.070	0.22	12.59	2.71	06:43:09:06	10.10.1978
59	33.622	57.040	0.14	09.89	1.66	16:40:50:93	10.10.1978
60	33.330	57.297	0.29	12.54	3.11	17:05:33:81	10.10.1978
61	33.289	57.225	0.30	04.18	1.48	00:27:15:10	11.10.1978
62	33.397	57.003	0.21	15.82	1.58	05:45:16:80	11.10.1978

located to find the areas of major activity. As a result of this, the geometry of the network was improved. The nine instruments were distributed and positioned in the manner shown in Figure 1 around the earthquake fault. This proved to be a good station distribution. Differences in station altitude are small and no corrections have yet been applied. The noise levels were generally low and most onset times could be read to within 0.1 sec. Over 200 shocks were recorded daily, yielding a total of about 6,000 recorded shocks. The 62 larger magnitude aftershocks were located and described here in order to give an overall and preliminary picture of the aftershock sequence.

Method of Location and Crustal Model

The velocity structure of the crust in the investigated area is not known. Therefore, we used the geological data to suggest a crustal velocity model. The first layer is composed of the Neogene clay deposits of 1 km thickness. This layer is underlain by about 6 km of lower Paleozoic to Mesozoic limestones with some sandstones. The lower Mid-Tertiary rocks are missing, and the lower Paleozoic rocks are underlain by Precambrian metamorphic rocks (Stocklin *et al.*, 1965; Stocklin and Nabavir, 1971; Aghanabati, 1975, 1977). The seismic compressional velocity values of 2.15 and 6.0 km/sec for clay (layer 1) and limestone (layer 2), respectively, given by Clark (1966) were used initially. These were later modified to minimize rms residuals in the hypocentral determinations. The model finally chosen for this *preliminary study* is a three-layered velocity model, of two flat layers over a half-space, with seismic compressional velocity values of 2.50, 5.00, and 6.00, respectively. The crustal model used by Crampin (1969) for epicentral determination of the nearby Dasht-e-Bayaz aftershocks (170 km ENE of Tabas) was tried, but gave large residuals.

For hypocentral location of the earthquakes, the modified form of Turcotte's (1964) computer program for a three-layer case is used. The location program starts with an initial location, the assumed three-layered crustal model, and improves the position by iteration. In all 62 cases presented in this study the iteration terminated by convergence. The hypocentral parameters together with standard errors of epicenters and focal depth are presented in Table 1.

Results and Discussion

The location of the 62 large magnitude aftershocks is presented in Figure 1. The seismic activity seems to be distributed along the fault with some clusters in the zones where there were no surface breaks. Similar features were seen in the Parkfield aftershock distribution (Eaton *et al.*, 1970). Unlike other aftershock sequences, none of the aftershocks is located at the extreme ends of the fault line. The overall distribution pattern of the aftershocks is asymmetric. They lie predominantly to the east of the mapped surface break, presumably on a thrust plane or planes dipping ENE. The epicenters are distributed in a band 25 km wide extending east of the westernmost mapped surface ruptures which lie at the edge of the Tabas playa. Thus the seismic deformation does not continue to the base of the Shotori horst (Figure 1). The larger aftershocks are distributed over 65 km along the length of the fresh faulting which accompanied the main shock.

The preliminary instrumental epicenter of the main shock by USGS, is reported as 33.145°N, 57.340°E with a focal depth of 42.1 km. This puts the instrumental epicenter of the main shock at the southeastern extremity of the surface ruptures. Even assuming 10 to 15 km in the location error of Iranian instrumental epicenters (Berberian, 1979c), it is still located at the southeastern extremity of the earthquake

fault. Therefore, either the rupture started from the southern end and propagated northward during the main shock, or the error of location is more than 15 km. If the USGS epicenter is to be relied on, a striking feature of the distribution of aftershocks located so far is that none of them is in the region of the main shock.

Table 1 shows that the deepest shock located was 24 km. About 45 per cent of the foci are at a depth between 5 to 10 km, 20 per cent between 10 to 15 km, 14 per cent between 2 to 5 km, 12 per cent between 15 to 20 km, and finally 4 per cent of the foci lie at a depth between 20 and 24 km. It therefore seems likely that the hypocentral

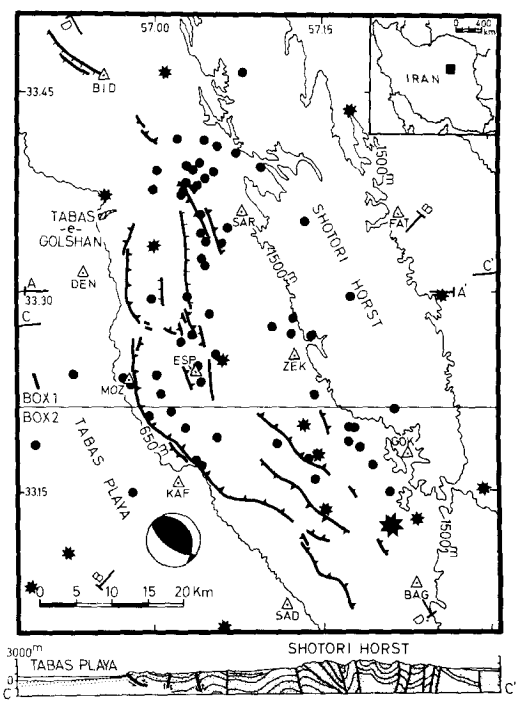

FIG. 1. Larger aftershocks and mapped surface ruptures of the Tabas-e-Golshan earthquake. Recording stations are marked by triangles and the aftershocks located in this paper are shown by small circles. The network operated for 30 days. ESP moved to KAF after 11 days and BAG to SAD after 3 days. Note the clusters that possibly indicate barrier zones of the main shock. AA′ and BB′ are the positions of the transverse cross sections in box 1 and 2, respectively, given in Figure 2, a and b. DD′ is the position of the longitudinal cross section parallel to the fault line given in Figure 2c. The geological cross section is along the line CC′. The random dashed-line pattern in the geological cross section represents pre-Neogene sedimentary rocks (mainly Paleozoic and Mesozoic limestones). The surface ruptures are shown by heavy barbed lines (triangle for thrust and short lines at right angles for high-angle reverse faults). Contour lines of 1500 m and 650 m above sea level indicate the boundaries of the Shotori compression horst and the Tabas compressional graben, respectively. The fault-plane solution of the main shock is also given. USGS reported epicenters of the main and larger aftershocks are shown by stars (based on the preliminary fault map of the Tabas-e-Golshan earthquake of 1978.09.16 after Berberian, 1979b).

depth of the main shock was shallower than 20 km. Teleseismic depth determinations are known to be inaccurate in Iran (Niazi *et al.*, 1978). Thus the teleseismic depth determination should not be regarded as being reliable.

Cross sections of the aftershock hypocenters are shown in Figure 2. Since the zone of surface ruptures changed strike from N–S to NW–SE at about 33°21′N latitude, the data are divided into two boxes (1 and 2 in Figure 1). Clearly, sections of this kind require that only hypocenters within a limited distance from the section should be projected. However, until more hypocenters are located, cross sections can only be made by projecting relatively long distances. On the basis of changes in strike of the surface breaks, the data in box 1 are projected onto the plane through

A-A′ (Figure 2a) and those in box 2 onto B-B′ (Figure 2b). The scatter of hypocenters in these sections may be attributed either to error in the projection process or to the presence of more than one active fault surface and of fault surfaces whose dip decreases with depth. Interpretations of the latter type are tempting (Chamberlain and Miller, 1918; Link, 1931; Rodgers, 1953; Fox, 1959; Badgley, 1965; Hamblin, 1965; Stewart, 1971; Proffett, 1977; and I.O.O.C.) but the data analyzed so far are insufficient to be conclusive. Broadly, the hypocenters are consistent with a main fault plane dipping at 40° to the ENE, which is in reasonable agreement with the observed dip of surface ruptures of about 30° (Berberian, 1979b). An analysis of the remaining data should resolve problems of this type.

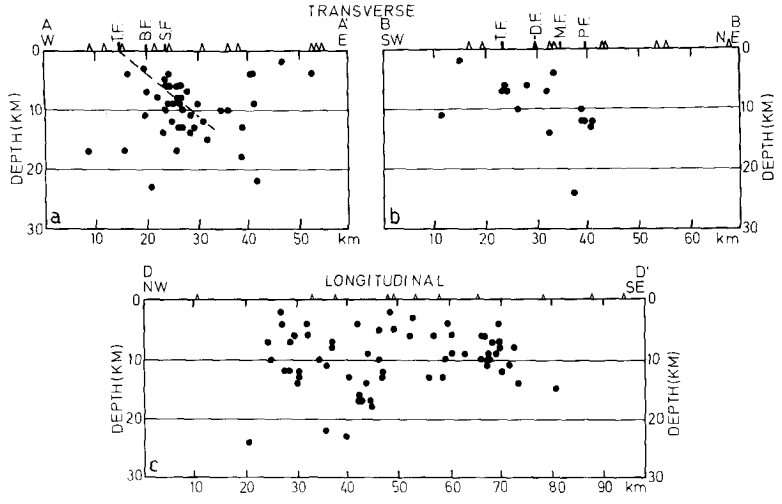

FIG. 2. Vertical cross sections of the seismicity of the Tabas area. (a) The hypocenters in box 1 (Figure 1) projected on the plane A-A′, perpendicular to the fault line oriented EW near 33°30′N latitude. (b) A similar projection from box 2 along plane B-B′ (Figure 1), oriented N40°E. (c) Longitudinal cross section with all data of Figure 1 (boxes 1 and 2) along plane D-D′, oriented N150°E. Positions of the stations and the earthquake faults are shown by triangles and thick short lines on the top of the cross sections. T.F., Tabas sole fault; B.F., S.F., D.F., M.F., and P.F. are other parallel earthquake fault segments (see Figure 1). Note the ENE dipping of hypocenters along earthquake thrust fault(s). The corresponding epicenters and the position of the section lines are given in Figure 1.

SOURCE PARAMETERS OF THE MAIN SHOCK

Based on the data collected from many seismological stations, a fault-plane solution was made for the main shock. The polarities of the *P*-wave first motion (Figure 3) show two nodal planes striking N152°E (dipping 31°NE) and N127°E (dipping 62°SSW). Field observations of the surface rupture indicate a thrust mechanism and indicate that the first plane is the fault plane.

The average trend of horizontal slip vectors for Early Quaternary thrust movements along the Tabas Fault, deduced from slickenside measurements on surface fault planes is N55°E with an average plunge of 40°NE (Berberian, 1979b), whereas the slip vector from the fault-plane solution of the 1978 earthquake has a trend of N36°E. This indicates a small change of slip vector trend from the early Quaternary to the recent deformation. However, the change is too small to change the basically thrust-type character of the fault. Larger changes in slip vector trends and hence the fault behavior since early Quaternary are already documented in Iran, which may indicate that evidence of early Quaternary movement cannot always provide a good clue to the present-day crustal deformation (Berberian *et al.*, 1979).

Based on the distribution of the aftershock sequence (assuming fault length L = 65 km and fault width W = 37 km) the seismic moment is $M_o = 16.2 \times 10^{26}$ dyne cm and the stress drop is $\Delta\sigma$ = 15 bars [using Kanamori and Anderson's (1975) relation for a thrust model]. This gives a higher seismic moment and a lower stress drop value compared with those calculated from field observations [$M_o(F) = 13.1 \times 10^{26}$ dyne cm and $\Delta\sigma(F)$ = 25 bars (Berberian, 1979b)].

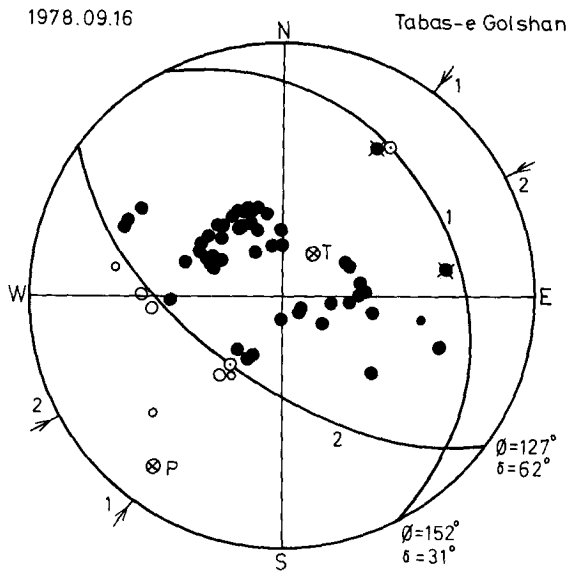

FIG. 3. Fault-plane solution of the Tabas-e-Golshan main shock of September 16, 1978. Equal area projection of the lower hemisphere of the focal sphere. Long-period polarity observations are shown as large circles and short-period data as small circles; open if the polarity was dilational, solid if it was compressional. T, tension axis; P, pressure axis. The foci are taken to be in the crust with a P-wave velocity of 6.8 km^{-1}. The horizontal projections of the slip vectors are shown by lines with arrows and numbers, outside the circle.

CONCLUDING REMARKS

Recognizing the limitations imposed by the small number of events located in this study, and the obvious complexity of the faulting indicated by the surface ruptures, some important questions about fault geometry and bedding plane slip remain unanswered. We expect to locate more than 3,000 recorded events to define the spatial and temporal distribution of activity. However, preliminary results indicate

1. That the main rupture possibly started at the southern end of the fault system and propagated north.
2. That the region of the main shock was not subsequently the source of large aftershocks.
3. No large aftershocks were located near the ends of the mapped surface faults.
4. Clusters of aftershocks occurred in regions where surface breaks were absent; thus, it is possible that these gaps extend to depth and acted as barriers during rupture (Das and Aki, 1977).
5. The aftershock distribution is asymmetrical with respect to the surface ruptures and broadly consistent with a fault plane or fault planes with an average dip of about 40° toward ENE.
6. The maximum depth of the aftershocks was 24 km. This suggests that the teleseismic depth estimate of 42 km for the main shock is in error.

7. Seismic moment and stress drop were estimated from field observation alone. They were $M_0(F) = 13.1 \times 10^{26}$ dyne cm and $\Delta\sigma(F) = 25$ bars (Berberian, 1979b). Using fault parameters determined from this aftershock study, new values of moment $M_0 = 16.2 \times 10^{26}$ dyne cm and stress drop $\Delta\sigma = 15$ bars are determined. This difference arises from changes in estimates of the depth and length of faulting. However, there is no good reason for supposing that the new values are more reliable than the earlier ones.

Acknowledgments

This work was supported by the Natural Environmental Research Council, the Royal Society of Great Britain, the consulting work of G. C. P. King and M. Berberian, the Department of Geodesy and Geophysics of Cambridge University, the United States Geological Survey, and the Geological and Mineral Survey of Iran. The 40-day expedition would not have been possible without enthusiastic cooperation from the Geological and Mineral Survey of Iran, who provided all the field support. We are grateful to Mr. R. Assefi, Managing Director, and Mr. J. Eftekharnezhad, Deputy Manager, of the Geological and Mineral Survey of Iran. We would like to thank G. C. P. King and D. P. McKenzie for critically reading the manuscript and for valuable discussions. Gratitude is also expressed to the Department of Geophysics, Imperial College, London, and Laboratoire Seismologique, Universite de Paris-sud, Centre d'Orsay, who at a very short notice lent us the recording instruments. We wish to thank the Directors of the WWSSN stations who kindly sent us a copy of their records for preparing the fault-plane solution of the main shock. The Department of Geophysics, Ferdowsi University of Mashad, kindly provided two more instruments which we operated during the last 16 days of the field study.

References

Aghanabati, A. (1975) Etude geologique de la region de Kalmard (W. Tabas): stratigraphic et tectonique, *Thesis*, Grenoble, 231 pp.

Aghanabati, A. (1977). Etude geologique de la region de Kalmard (W. Tabas): stratigraphic et tectonique, *Geol. Surv. Iran* **35,** 230 pp.

Badgley, P. C. (1965). Structural and tectonic principles, Harper and Row, New York, 521 pp.

Berberian, M. (1976). An explanatory note on the first seismotectonic map of Iran: a seismotectonic review of the country, *Geol. Surv. Iran* **39,** 7–142.

Berberian, M. (1979a). Tabas-e-Golshan (Iran) catastrophic earthquake of 16 September 1978: a preliminary field report, *Disaster* **2,** 207–219.

Berberian, M. (1979b). Earthquake faulting and bedding thrust associated with the Tabas-e-Golshan (Iran) earthquake of September 16, 1978, *Bull. Seism. Soc. Am.* **69,** 1861–1887.

Berberian, M. (1979c). Evaluation of the instrumental and relocated epicentres of Iranian earthquakes, *R. Astr. Soc.* **58,** 625–630.

Berberian, M., I. Asudeh, and S. Arshadi (1979). Surface rupture and mechanism of the Bob-Tangol (SE Iran) earthquake of 19 December 1977, *Earth Planet. Sci. Letters* **42,** 456–462.

Chamberlain, R. T. and W. Z. Miller (1918). Low-angle faulting, *J. Geol.* **26,** 1–44.

Clark, S. P., Jr. (Editor) (1966). Handbook of physical constants (Rev. ed.), *Geol. Soc. Am. Mem.* **79,** New York, 630 pp.

Crampin, S. (1969). Aftershocks of the Dasht-e-Bayas, Iran, earthquake of August 1968, *Bull. Seism. Soc. Am.* **59,** 1823–1841.

Das, S. and K. Aki (1977). Fault plane with barriers: a versatile earthquake model, *J. Geophys. Res.* **82,** 5658–5670.

Eaton, J. P., W. H. K. Lee, and L. C. Parkiser (1970). Use of microearthquakes in the study of the mechanics of earthquake generation along the San Andreas Fault in central California, *Tectonophysics* **9,** 259–282.

Fox, F. G. (1959). Structure and accumulation of hydrocarbons in southern foothills, Alberta, Canada, *Bull. Am. Assoc. Petrol. Geol.* **43,** 992–1025.

Hamblin, W. K. (1965). Origin of reverse drag on the downthrown side of normal faults, *Bull. Geol. Soc. Am.* **76,** 1145–1164.

I.O.O.C., Iranian Oil Operating Companies. Geological maps of Zagros Mountains, scale 1:100,000. Geological and Exploration Division, Tehran.

Kanamori, H. and D. L. Anderson (1975). Theoretical basis of some principal relations in seismology, *Bull. Seism. Soc. Am.* **65,** 1073–1095.

Link, T. A. (1931). Individualism of orogenies suggested by experimental data, *Bull. Am. Assoc. Petrol. Geol.* **15,** 325–403.

Niazi, M., I. Asudeh, G. Ballard, J. Jackson, G. King, and D. McKenzie (1978). The depth of seismicity in the Kermanshah region of the Zagros Mountains (Iran), *Earth Planet. Sci. Letters* **40,** 270–274.

Proffett, J. M., Jr. (1977). Cenozoic geology of the Yerington district, Nevada, and implications for the nature and origin of Basin and Range faulting, *Bull. Geol. Soc. Am.* **88,** 247–266.

Rodgers, J. (1953). The folds and faults of the Appalachian Valley and Ridge province, Southeastern Symposium, 1950, *Kentucky Geol. Surv., Ser. 9, Spec. Publ.* **1,** 150–166.

Stewart, J. H. (1971). Basin and Range structure: a system of horsts and grabens produced by deep-seated extension, *Bull. Geol. Soc. Am.* **82,** 1019–1044.

Stocklin, J., J. Efterkharnezhad, and A. Hushmandzadeh (1965). Geology of the Shotori Range (Tabas area, eastern Iran), *Geol. Surv. Iran* **3,** 68 pp.

Stocklin, J. and M. H. Nabavir (compilers) (1971). Explanatory note of the Bushruyeh Quadrangle map, 1:250,000. *Geol. Surv. Iran* J7.

Turcotte, F. T. (1964). Epicenters and focal depths in the Hollister region of central California, *Ph.D. Thesis*, University of California, Berkeley.

DEPARTMENT OF GEODESY AND GEOPHYSICS
UNIVERSITY OF CAMBRIDGE
MADINGLEY RISE, MADINGLEY ROAD
CAMBRIDGE CB3 OEZ ENGLAND (M.B., I.A., C.S.)

LAMONT-DOHERTY GEOLOGICAL OBSERVATORY
OF COLUMBIA UNIVERSITY
PALISADES, NEW YORK 10964 (R.G.G., C.H.S.)
CONTRIBUTION NO. 2908

Manuscript received March 20, 1979